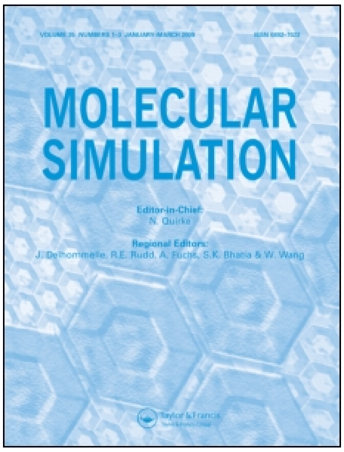

Molecular Simulation
Publication details, including instructions for authors and subscription information:
http://www.informaworld.com/smpp/title~content=t713644482

The adsorption of poly (vinyl alcohol) on the hydroxylated β-cristobalite

Dan Mu[a]; Xu-Ri Huang[a]; Chia-Chung Sun[a]
[a] State Key Laboratory of Theoretical and Computational Chemistry, Institute of Theoretical Chemistry, Jilin University, Changchun, China

To cite this Article Mu, Dan , Huang, Xu-Ri and Sun, Chia-Chung(2008) 'The adsorption of poly (vinyl alcohol) on the hydroxylated β-cristobalite', Molecular Simulation, 34: 6, 611 — 618
To link to this Article: DOI: 10.1080/08927020801993354
URL: http://dx.doi.org/10.1080/08927020801993354

Molecular Simulation
Vol. 34, No. 6, May 2008, 611–618

Taylor & Francis
Taylor & Francis Group

The adsorption of poly (vinyl alcohol) on the hydroxylated β-cristobalite

Dan Mu, Xu-Ri Huang* and Chia-Chung Sun

State Key Laboratory of Theoretical and Computational Chemistry, Institute of Theoretical Chemistry, Jilin University, Changchun 130023, China

(*Received 13 July 2007; final version received 14 February 2008*)

The adsorption of poly (vinyl alcohol) with different chain lengths on a hydroxylated β-cristobalite (100) surface is studied *via* molecular simulations. The relative dielectric constant is selected to be 1 and 78 to mimic in vacuum and in solution environment, respectively. Different configurations and dynamic properties are found in the two absolutely different environments, showing that the solvent condition plays an important role in the process of chain adsorption and diffusion on a surface. In equilibrium, the chain possesses (partial) ordered configuration in vacuum condition.

Keywords: molecular dynamics simulation; PVA; β-cristobalite surface; adsorption; ordered configuration

1. Introduction

The behaviour of polymers at the liquid–solid interface is crucial to technologies involving molecular surface placement [1,2]. Polymers adsorbed onto a surface to form thin films is an emerging topic of modern materials science [3,4]. They can be applied, for example, in the fields of biosensors, light-emitting diodes, nonlinear optical devices and permeation-selective gas membranes [5–10]. The fabrication of the thin films always takes place in vacuum or dilute solutions. The adsorption of the polymer chains can be controlled by varying multiple parameters such as the polymer-surface interaction, the solvent quality, surface nano-roughness, temperature, polymer chain length and so on. The knowledge about the adsorption dynamics and the thermodynamics of the equilibrium adsorption is crucial to understand and furthermore improve the property of the final product. Experimentally it is difficult to control the above influences well separately; thus, clear information on the exact effect of a specific environmental parameter is hard to obtain. Due to the fast-growing computation power nowadays, it is possible to utilise the computer as an ‘experimental apparatus’ to solve the problem, with the aid of various simulation techniques.

Binder and coworkers successfully studied polymer films in different conditions *via* computer simulations [11–14]. Briggman et al. studied the free surface of polystyrene thin film on oxidised Si substrates. By simulation, they found that phenyl groups point outwards away from the surface [15]. Lu and Kim observed the surface pattern of a thin polymer film by using a three-dimensional (3D) electrostatic model. The competition between the electrostatic energy and the surface energy leads to a characteristic pillar size. Furthermore, the film thickness significantly influences the growth rate and the distance between pillars [16]. Recently, Kumar and coworkers found that a non-wetting solvent aids adsorption of the polymer chain at low sticking energies compared to wetting solvent by the aid of molecular dynamics simulations [17].

In most of the simulations that focus on the physical adsorption of polymer chains, the structure of the solid surface is always taken as frozen. Among these adsorption surfaces, there are a lot of surfaces in application that possess dangling hydroxyl groups or charges. The adsorption of hydrophilic polymers on these surfaces is very strong, due to special interactions such as hydrogen bond or charge transfer. Therefore the frozen surface model is not suitable in these cases. Moreover, the distribution of the hydroxyl groups on the surface may strongly influence the chain dynamics because the hydrogen bonds are directional. An important example is the β-cristobalite surface, which is always used in applications. Its (100) and (111) surfaces are in general supposed to be the representations of the silica surface. They are easily hydroxylated so that the surfaces are full of dangling hydroxyl groups. The adsorption of polymer chain containing hydroxyl groups on the hydroxylated β-cristobalite (100) surface is very interesting: due to the strong interaction the polymer chain may behave totally differently.

---

*Corresponding author. Email: huangxuri2005@yahoo.com.cn

ISSN 0892-7022 print/ISSN 1029-0435 online

DOI: 10.1080/08927020801993354
http://www.informaworld.com

Poly(vinyl alcohol) (PVA) is one of the simplest polymer chains containing hydroxyl groups. Knowing its adsorption behaviour on such a surface may help us to understand and control the adsorption behaviour of similar polymers containing hydroxyl side groups but with comparatively complicated structures. The polymer in dilute solution can be well modelled as a single molecule in a simulation box, which does not interact with the nearby neighbours. Here we study the equilibrium configurations and dynamic properties of a single PVA chain with various chain lengths in the adsorption processes *via* molecular dynamics simulation. The solvent quality is varied to see its influence on the adsorption dynamics and configuration. In a vacuum, the PVA chain is strongly attached to the surface, and therefore its mobility is severely reduced. Moreover, the surface plays the role of a template, so that the chain is always adsorbed directionally along (110). Above a critical chain length, the adsorbed PVA chain is folded back, showing a less ordered structure. In solution, there is no such ordered chain configuration. The number of the hydrogen bonds between the surface and the PVA chain is largely reduced.

2. Model and simulation details

The simulation processes are all carried out at room temperature (298 K) with Molecular Simulation (MD) procedure of the Cerius2 package program on SGI work station. We adopt the (100) surface of β-cristobalite as a hydrophilic surface, which is modelled by a slab geometry with 3D periodic boundary conditions. This surface is with ordered hydroxyl construction and free of defect [18], since it is cut from the β-cristobalite perfect crystal with 11 atom-layer thick [19]. The slabs are separated by 70Å, which is large enough to ignore the interaction between the adjacent slabs in Z direction. The dangling bonds on top and bottom surfaces are saturated by hydrogen atoms, therefore the top surface is changed to be hydroxylated [20]. We build up the surface large enough so that the adsorbed PVA chain cannot interact with its neighbouring images in XY plane. PVA chains with degree of polymerisation $N = 10$, 20, 30, 50 and 60 are considered in the simulations. The corresponding simulation boxes adopt 57.68Å × 57.68Å × 70Å for the former two chain lengths, and 86.52Å × 86.52Å × 70Å for the latter three chain lengths. However, the surface hydroxyl concentration is constant, that is, $1.278 \times 10^{-5}\,\mathrm{mol/m^2}$.

The energy minimisation is first performed to relax the chain and surface unfavorable structures. Then the molecular dynamics simulation is carried out at 300 K with Nosé-Hoover [21] thermostat in canonical ensemble. The COMPASS force field [22–24], which was recently developed to high accuracy, is used to describe the atom–atom interactions at fully atomistic level. The COMPASS forcefield adopts a set of complex potential functions. The energy expression comprises a combination of valence terms, including diagonal and cross-coupling terms for bond stretching, bond angle bending and dihedral angle distortions. For van der Waals interactions, we adopt the spline treatment, and the spline window is between 11 and 12Å. The Ewald summation [25] is applied to calculate long range electrostatic interactions, which is important in our simulation that includes so many hydroxyl groups. The Verlet leapfrog algorithm [26] is used to integrate the equations of motion with a time step of 1 fs. Each simulation runs at least for 1 ns. The surface hydroxyl groups are free to move in the simulations, whereas the silicon and oxygen atoms below them are constrained and unmovable.

3. Simulation results and discussion

We first study the chain adsorption in vacuum. PVA chains with different lengths ranging from 10 to 60 are considered, with their initial configuration generated *via* Monte Carlo. Figure 1 shows the distance H_d between the mass centre of PVA and the surface during the simulation for $N = 30$. The variation of H_d with time reflects the adsorption dynamics. It can be clearly seen that after about 357 ps the PVA chain is well adsorbed onto the surface, and H_d only fluctuates around 2.5Å. At the beginning of the simulation, the PVA chain approaches to the surface in a few ps. Several hydrogen bonds are formed between the surface and the part of chain which is near the surface. After that the chain slowly adjusts its configuration and position to lower the total energy. In this process the chain changes from random coil-like to extended structure. However, some of the segments in the middle of the chain cannot form hydrogen bonds with the

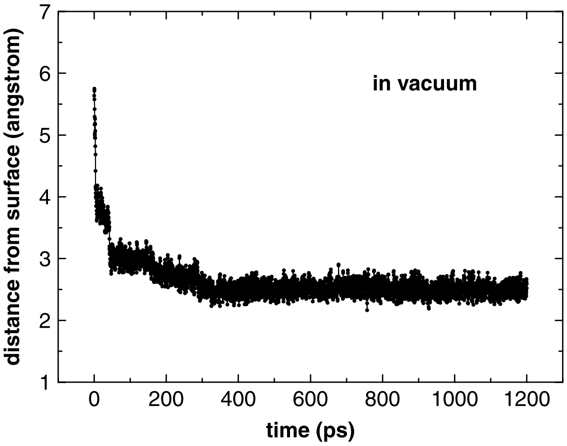

Figure 1. The distance of the mass centre of PVA with $N = 30$ from the surface, where N is the degree of polymerisation of PVA chain.

surface hydroxyl groups because the nearby segments have already formed hydrogen bonds with the surface. These segments are forced to stay above the adsorption layer, thus the distance between the chain mass centre and the surface is larger than 3.5Å. The 'lump' formed by these segments moves towards the chain ends during the simulation and finally disappears. Then the whole chain approaches the surface, again in a few ps, to maximise the surface–chain attractive interaction. The chain adjusts its configuration and slowly approaches the surface till H_d reaches an equilibrium value. For PVA with other chain lengths, the adsorption dynamics is similar, except for PVA with larger chain lengths whose 'lump' can not be transferred to the chain ends in the simulation time. Take $N = 30$ case for example, we show such adsorption process in Figure 2 and its corresponding configurations during the adsorption process are also presented.

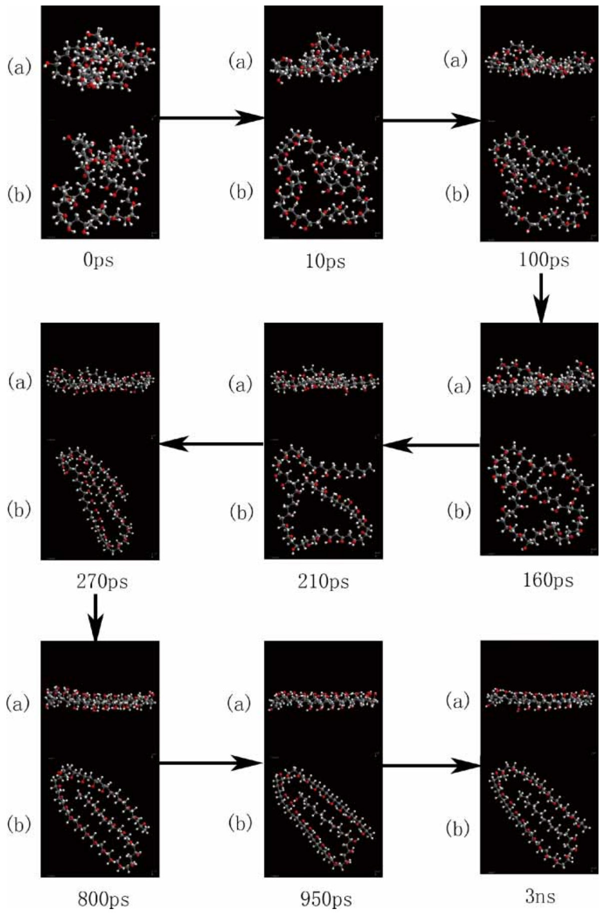

Figure 2. In this figure (a) shows the side view of the polymer chain models in vacuum. (b) the top view. The hydroxylated β-cristobalite (100) surface is not displayed for simplicity. The red color denotes O, the grey C, and the light grey H.

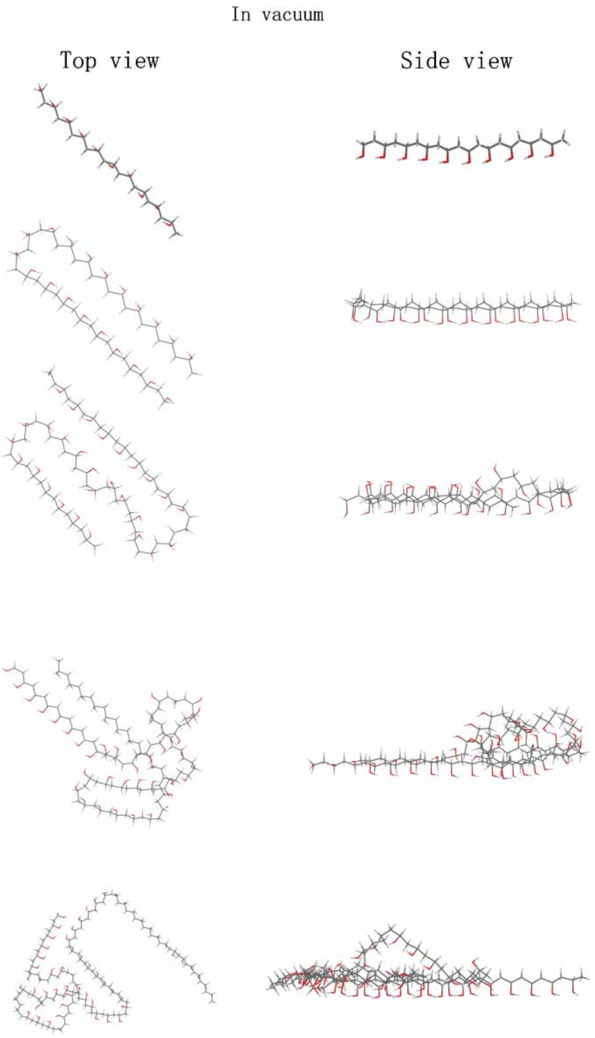

Figure 3. The top and side view of the PVA chain with $N = 10$, 20, 30, 50, and 60, respectively. The image capture angles of snap shots of PVA configurations from top and side view are the same as surface (b) and (a) in Figure 2, respectively.

After equilibrium, the chain is adsorbed onto the hydroxylated silica surface with an apparently regular local pattern as shown in Figure 3. Moreover, the chain is globally oriented along surface (110) direction. The orientation parameter P_2 is defined *via*

$$P_2 = \frac{3 < \cos^2(\theta) > -1}{2},$$

where θ is the angle between the sub-bond vector of the adjacent C-C bonds and the (110) direction. $P_2 = 1$ means that the chain is totally parallel to (110), $P_2 = -0.5$ totally perpendicular to (110), and $P_2 = 0$ no global chain orientation preferences. Figure 4 shows the calculated P_2 for different chain length of PVA. The value of P_2 is near to 1.0 for $N = 10$, and in general it decreases with increasing N. This reflects the fact that there are more folds and random oriented parts of the chain with increasing chain length. However, P_2 is larger

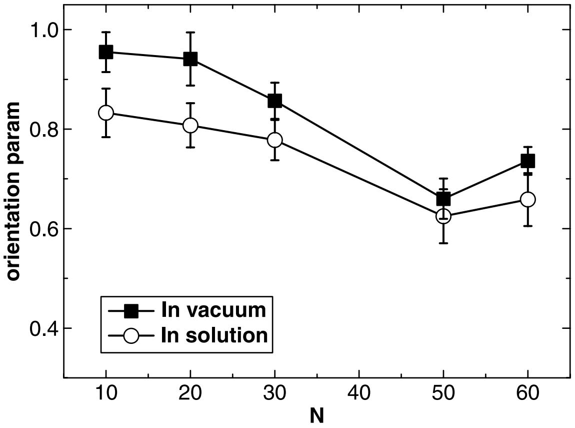

Figure 4. The chain orientation parameter along (110) both in vacuum and with solvent effects.

for $N = 60$ than $N = 50$. The PVA with such long chain length is no more two dimensionally but three dimensionally adsorbed onto the surface, which is due to stronger interaction between the chain units in comparison with the attractive interaction between chain and surface. From the snapshot of $N = 60$ we can see that some parts of the chain are oriented along surface (110) but some parts show no orientation preference compared with the $N = 50$ case. The equilibrium adsorption configuration is highly correlated to the initial chain configuration. Due to the fast adsorption process, more PVA segments are 'frozen' above the first adsorption layer, correspondingly P_2 is smaller. The chain–surface interaction is very strong, therefore the adsorbed chain configuration is not easy to change. In atomic force microscopy experiments, the chain is normally supposed to be two dimensionally adsorbed [27]. Our simulation results imply that for a polymer which is strongly attracted to the surface with sufficient chain length, it is difficult to be adsorbed onto the surface two dimensionally because the adsorption configuration is quenched.

The adsorbed chain configuration is extended and possesses folded structure for $N > 20$. Such a partial order due to adsorption is interesting, because it might be related to the production of high performance functional thin film which require ordered chain arrangement that enhance electron transfer. For $N = 10$ and 20, most of the PVA hydroxyl groups form hydrogen bonds with surface, and only several intra-chain hydrogen bonds exist. For $N = 30$, it is very interesting that the first fold of the molecule forms hydrogen bonds with the surface, whereas the third fold totally forms intra-chain hydrogen bonds. A comparison between the equilibrium configuration of $N = 20$ and $N = 30$ is shown in Figure 5. The molecules with longer chain lengths possess more intra-chain hydrogen bonds [28] and consequently possess certain height in Z direction, although some parts of the molecule are oriented along (110) due to the formation of PVA-surface hydrogen bonds. It seems that for short chain length, the hydroxylated surface plays the role of a template to induce PVA preferential adsorption along (110). In order to see the effect of the surface as a template, we also simulated the adsorption of PVA with $N = 20$ starting from different initial configurations. It was found that the chain is possibly adsorbed on the surface along $(1\bar{1}0)$ after equilibrium. In order to explain such an extraordinary phenomenon, we calculated the adsorption energy for $N = 20$ chain with its whole configuration unchanged, only its direction turned to (110), and calculated its adsorption energy, but its corresponding adsorption energy was about 10 kcal/mol lower than that of adsorption along $(1\bar{1}0)$. In this case, simulating for a longer time would not change the chain global orientation from $(1\bar{1}0)$ to (110), which implies a substantial activation energy barrier between these two adsorption states.

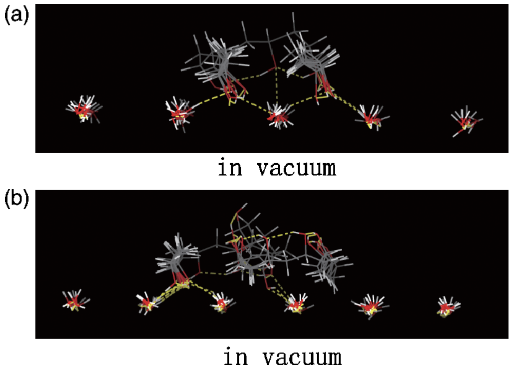

Figure 5. The orderly folded equilibrium structures of PVA with (a) $N = 20$ and (b) 30, respectively. Only parts of the hydroxyl groups of the surface are shown. The two folds of $N = 20$ mainly form hydrogen bonds with surface. Interestingly, the third fold of $N = 30$ only forms intra-chain hydrogen bonds. The red color denotes O, the white H, and the grey C. The yellow dash lines are for the hydrogen bonds.

Figure 6(a) and (b) show the adsorption energy (*E*) and the adsorption energy per segment (*E*/*N*) with increasing chain length, respectively. The PVA chain is adsorbed stronger on the surface with increasing chain length. However the chain configuration is less ordered for larger *N* and possesses certain height in *Z* direction, thus the adsorption energy per segment is smaller with increasing *N*, approaching an asymptotic value. The dependence of the adsorption energy on the chain length reflects the configuration variation during adsorption. Suppose that the chain is adsorbed onto the surface with extended configuration along (110), then the adsorption energy should increase proportionally with increasing *N*. Its average per segment should possess the same value, which is mainly attributed to the energy

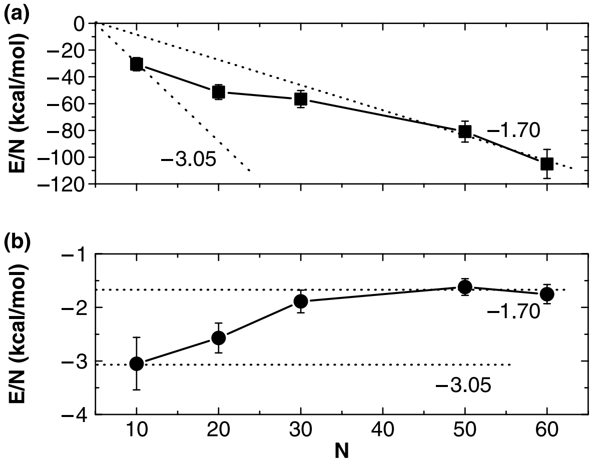

Figure 6. The adsorption energy E in vacuum and the adsorption energy per segment E/N in vacuum are shown in (a) and (b), respectively. The dotted line with slope -3.05 is the asymptotic line for totally extended chain adsorption. Another dotted line with slope -1.70 is the asymptotic line for the adsorption with longer chain length.

of the hydrogen bond formation between one segment and the surface. In this situation E should increase with N linearly with a slope -3.05 as shown by the dotted line in Figure 6(a). However in the simulations, the adsorption energy does not increase proportionally to N and its average per segment is not a constant. Actually, for longer chain lengths, E/N approaching an asymptotic value is also reasonable: E is proportional to the area of the contact surface S, which is proportional to R_g^2. For bulk system R_g^2 is proportional to N, thus E is proportional to N. This characteristic relation between E and N is reflected by the dotted line in Figure 6 with a slope of -1.70 for longer chain length. The nonlinear variation of the adsorption energy per segment between -3.05 and -1.70 with increasing N corresponds to the chain configuration changing from extended to partially random. After reaching adsorption equilibrium, PVA with intermediate chain length takes the folded configuration. This is the result of competition between intra-chain and chain–surface interactions. We can estimate the intra-chain interaction energy by comparing the energy difference between the chain with extended and that with folded configuration. Figure 7 shows the calculated intra-chain and chain–surface interaction energies with increasing chain length. Apparently the intra-chain energy is always larger than the chain–surface interaction energy for $N > 20$. Correspondingly, the chain prefers the folded configuration for N larger than a critical value. Suppose a linear relationship between the calculated interaction energy and the chain length, we may extrapolate the two lines towards shorter chain length and obtain a crossover at $N = 13$. This is the rough estimation of the critical chain length above which the chain prefers a folded configuration. To see if this estimation is correct or not, we further simulate a system with $N = 15$. After adsorption equilibrium we also find a folded structure.

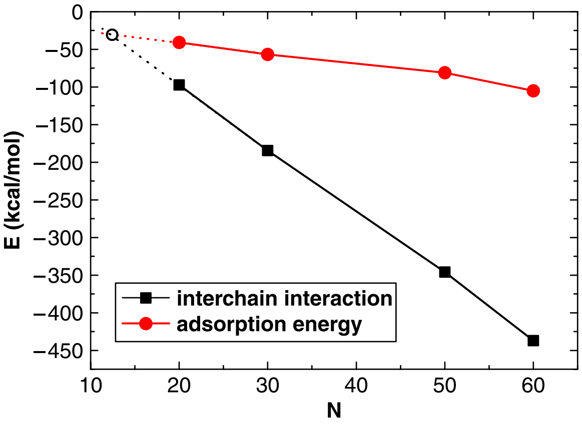

Figure 7. The intra-chain and the chain–surface interaction energies in vacuum with increasing chain length.

The self-diffusion coefficient (D) of the adsorbed chain can be calculated from the mean square displacement *via* Einstein relation. Figure 8 shows the calculated D for PVA with different chain lengths in vacuum and in solution. In general, D decreases with increasing N. For $N = 10$, the calculated D is much larger than that of other chain lengths, which approaches zero when $N > 20$. This reflects the strong surface–chain interaction so that the PVA chain is no longer able to move freely.

We set the relative dielectric constant to 78 to mimic the 'in solution' [29,30] condition. Though there are some differences in the results by treating the solvent with the implicit or the explicit model [31], we opt to take the implicit solvent model in order to save

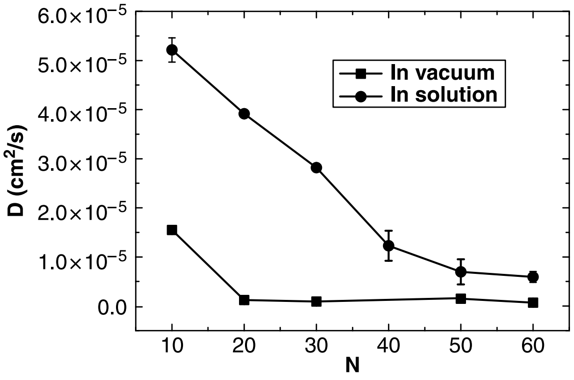

Figure 8. The chain self diffusion coefficient is shown in the case of vacuum and solution condition, respectively.

simulation time. What we aim to study is the solvent effect on the adsorption and diffusion process of the PVA chain on the surface, not to obtain quantitative relations. Simply changing the solvent dielectric constant can supply fundamental information to understand the effects of solvent on the chain adsorption behaviour. In Figure 8 we have compared the PVA diffusion coefficients calculated for the vacuum and 'in solution' conditions, respectively. It is shown that the chain mobility in solution is largely enhanced. For larger N, the diffusion coefficient D is even one order larger in magnitude for the chain in solution than that in vacuum.

The chain equilibrium configuration after adsorption in solution is interesting, because in real experiments the layer by layer assembly depends largely on the adsorbed chain configuration. In Figure 9 we compare the equilibrium configurations of PVA chain with $N = 10$ in vacuum and in solution, respectively. In contrast to the chain configuration of PVA in vacuum, the configuration of PVA in solution is not linearly stretched. Moreover, the chain in solution does not orient along the (110) direction and does not possess any dominant orientation in comparison to that in vacuum. From the side view, there are no surface–polymer hydrogen bonds for the chain in solution. Even the chain has the tendency to be desorbed from the surface. It should be noted that our simulation conditions correspond to the dilute solution in which the molecules can be adsorbed separately.

In Figure 10 the configuration of PVA with $N = 60$ is shown for that 'in solution' case. Compared to Figure 3(e), the chain in solution is totally adsorbed on the surface. This is very interesting because intuitively one may suppose that the hydrophilic PVA chain will be easily desorbed from the surface in solution. The parts of

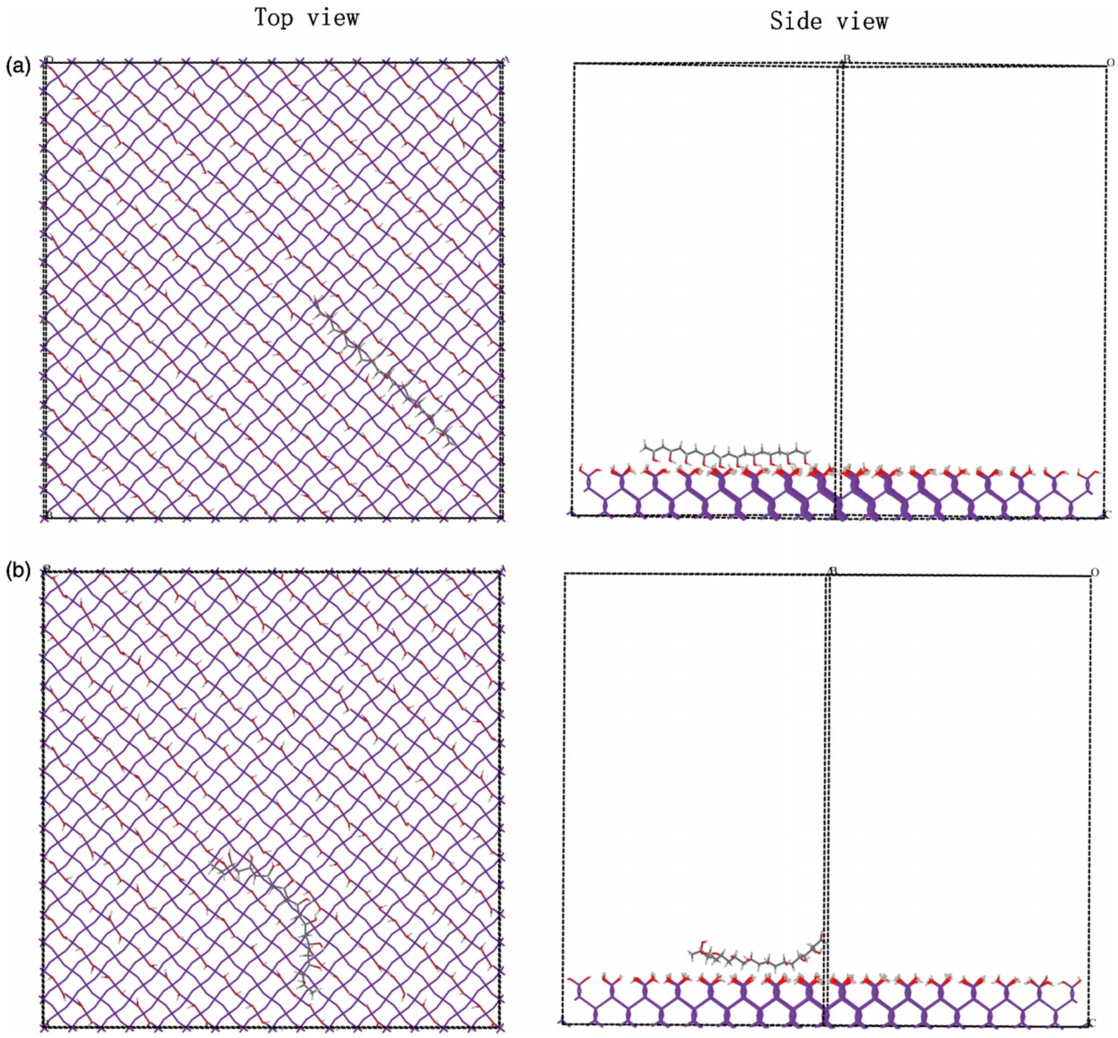

Figure 9. The top and side view of the PVA chain with $N = 10$ in vacuum and solution, respectively. The purple color denotes Si, the red O, the grey C, and the light grey H.

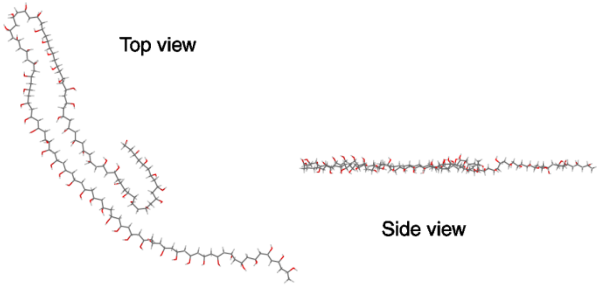

Figure 10. The top and side view of the PVA chain with $N = 60$ in solution.

the chain are not oriented along a specific direction, and there are only several surface–polymer hydrogen bonds. The reason that the chain is still well adsorbed on the surface in solution is due to the van der Waals interaction. ecause the strong surface–polymer hydrogen bonds are broken in solution, the parts of the chain can adjust their positions more easily. Thus, in equilibrium, the chain possesses two-dimensional adsorption configuration. Comparing the PVA adsorption in solution with different chain lengths, we find that shorter chains are easier to be desorbed, which is in agreement with real experiments.

4. Conclusion

In this paper, we study the adsorption of a typical hydrophilic chain on a strong hydrophilic surface where hydrogen bonds can form between them. The vacuum and 'in solution' conditions are considered separately, and the effects of molecular weight on the adsorption behaviour are taken into account. For short chains in vacuum, the adsorbed molecule configuration is ordered and the molecule is oriented along (110). Increasing the molecular weight to a moderate extent, the molecule possesses folded configuration and the whole molecule is still oriented along (110). Therefore we show the possibility of producing ordered single polymer layer and suggest control factors. When the molecular weight is large enough, the adsorbed molecule configuration is frozen with certain height in the Z direction, i.e. not easy to change due to the strong surface-polymer interactions. In solution, there is no orientation preference of the molecules and the configurations are always two-dimensional and not ordered, no matter what the molecular weight is. Furthermore, the mobility of the molecules in solution is larger than that in vacuum, which implies that the molecules in solution is easier to be desorbed. These results may relate to the experiments of template-induced self-assembly of molecules.

References

[1] C.A. Haynes and W. Norde, *Globular proteins at solid/liquid interfaces*, Colloids. Surf. B 2 (1994), pp. 517–566.

[2] M. Malmsten, *Formation of adsorbed protein layers*, J. Colloid. Interface. Sci. 207 (1998), pp. 186–199.

[3] G. Decher, *Fuzzy nanoassemblies: Toward layered polymeric multicomposites*, Science 277 (1997), pp. 1232–1237.

[4] A.R. Esker, C. Mengel, and G. Wegner, *Ultrathin films of a polyelectrolyte with layered architecture*, Science 280 (1998), pp. 892–895.

[5] F. Caruso, R.A. Caruso, and H. Mohwald, *Nanoengineering of inorganic and hybrid hollow spheres by colloidal templating*, Science 282 (1998), pp. 1111–1114.

[6] S.S. Shiratori and M.F. Rubner, *pH-dependent thickness behavior of sequentially adsorbed layers of weak polyelectrolytes*, Macromolecules 33 (2000), pp. 4213–4219.

[7] S.L. Clark and P.T. Hammond, *Engineering the microfabrication of layer-by-layer thin films*, Adv. Mater. 10 (1998), pp. 1515–1519.

[8] M. Husemann, M. Morrison, D. Benoit, J. Frommer, C.M. Mate, W.D. Hinsberg, J.L. Hedrick, and C.J. Hawker, *Manipulation of surface properties by patterning of covalently bound polymer brushes*, J. Am. Chem. Soc. 122 (2000), pp. 1844–1845.

[9] Y.N. Xia and G.M. Whitesides, *Soft lithography*, Annu. Rev. Mater. Sci. 28 (1998), pp. 153–184.

[10] W.T.S. Huck, A.D. Strook, and G.M. Whiteside, *Synthesis of geometrically well defined, molecularly thin polymer films*, Angew. Chem. Int. Ed. Engl. 39 (2000), pp. 1058–1061.

[11] A. Milchev and K. Binder, *Dewetting of thin polymer films adsorbed on solid substrates: A Monte Carlo simulation of the early stages*, J. Chem. Phys. 106 (1997), pp. 1978–1989.

[12] R.B. Pandey, A. Milchev, and K. Binder, *Semidilute and concentrated polymer solutions near attractive walls: Dynamic monte carlo simulation of density and pressure profiles of a coarse-grained model*, Macromolecules 30 (1997), pp. 1194–1204.

[13] F. Varnik, J. Baschnagel, K. Binder, and M. Mareschal, *Confinement effects on the slow dynamics of a supercooled polymer melt: Rouse modes and the incoherent scattering function*, Eur. Phys. J. E. 12 (2003), pp. 167–171.

[14] Y.-C. Lin, M. Müller, and K. Binder, *Stability of thin polymer films: Influence of solvents*, J. Chem. Phys. 121(8) (2004), pp. 3816–3828.

[15] K.A. Briggman, J.C. Stephenson, W.E. Wallace, and L.J. Richter, *Absolute molecular orientational distribution of the polystyrene surface*, J. Phys. Chem. B 105 (2001), pp. 2785–2791.

[16] D.-C. Kim and W. Lu, *Three-dimensional model of electrostatically induced pattern formation in thin polymer films*, Phys. Rev. B 73 (2006), p. 035206.

[17] T. Desai, P. Keblinski, and S. Kumar, *Computer simulations of the conformations of strongly adsorbed chains at the solidCliquid interface*, Polymer 47 (2006), pp. 722–727.

[18] J. Du and A. Cormack, *Molecular dynamics simulation of the structure and hydroxylation of silica glass surfaces*, J. Am. Ceram. Soc. 88(10) (2005), p. 2978.

[19] S. Iarlori, D. Ceresoli, M. Bernasconi, D. Donaldio, and M. Parrinello, *Dehydroxylation and silanization of the surfaces of (-cristobalite silica: An ab initio simulation*, J. Phys. Chem. B 105 (2001), pp. 8007–8013.

[20] Z.Y. Lu, Z.Y. Sun, and Z.S. Li, *Stability of two-dimensional tessellation ice on the hydroxylated beta-cristobalite (100) surface*, J. Phys. Chem. B 109(12) (2005), pp. 5678–5683.

[21] W.G. Hoover, *Canonical dynamics: Equilibrium phase-space distributions*, Phys. Rev. A 31 (1985), pp. 1695–1697.

[22] H. Sun, *COMPASS: An* ab initio *force-field optimized for condensed-phase applications-overview with details on alkane and benzene compounds*, J. Phys. Chem. B 102 (1998), pp. 7338–7364.

[23] H. Sun, P. Ren, and J.R. Fried, *The COMPASS force field: Parameterization and validation for phosphazenes*, Comput. Theor. Polym. Sci. 8 (1998), pp. 229–246.

[24] D. Rigby, H. Sun, and B.E. Eichinger, *Computer simulations of poly (ethylene oxide): Force field, pvt diagram and cyclization behaviour*, Polym. Int. 44 (1997), pp. 311–330.

[25] P.P. Ewald, *Die Berechnung optischer und elektrostatischer Gitterpotentiale*, Ann. Phys. 64 (1921), pp. 253–287.

[26] L. Verlet, *Computer 'experiments' classical fluids. I. thermodynamical properties of Lennard-Jonesmolecules*, Phys. Rev. 159 (1967), pp. 98–103.

[27] Y. Roiter and S. Minko, *Adsorption of polyelectrolyte versus surface charge:* In situ *single-molecule atomic force microscopy experiments on similarly, oppositely, and heterogeneously charged surfaces*, J. Phys. Chem. B 111(29), pp. 8597–8604.

[28] Ph. Wernet, D. Nordlund, U. Bergmann, M. Cavallieri, M. Odelius, H. Ogasawara, L.A. Näsland, T.K. Hirsch, L. Ojamäe, P. Glatzel et al., *The structure of the first coordination shell in liquid water*, Science 304 (2004), pp. 995–999.

[29] X.L. Wang, Z. Lu, Z.S. Li, and C.C. Sun, *Molecular dynamics simulation study on adsorption and diffusion processes of a hydrophilic chain on a hydrophobic surface*, J. Phys. Chem. B. 109(37) (2005), pp. 17644–17648.

[30] M. Rubinstein and R.H. Colby, *Polymer Physics*, Oxford University Press, Oxford, 2003.

[31] G. Reddy and A. Yethiraj, *Implicit and explicit solvent models for the simulation of dilute polymer solutions*, Macromolecules 39(24) (2006), pp. 8536–8542.